Marine Chemistry 273 (2025) 104571

Contents lists available at ScienceDirect

Marine Chemistry

journal homepage: www.elsevier.com/locate/marchem

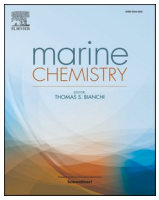

Acid-leachability of metals from suspended particles in the Pacific Ocean

Yoshiki Sohrin [a,*], Linjie Zheng [a], Cheuk-Yin Chan [a], Yuzuru Nakaguchi [b], Shotaro Takano [a], Rumi Sohrin [c], Wen-Hsuan Liao [d], Tung-Yuan Ho [e]

[a] Institute for Chemical Research, Kyoto University, Gokasho, Uji, Kyoto 611-0011, Japan
[b] School of Science and Engineering, Kindai University, Kowakae, Higashiosaka, Osaka 577-8502, Japan
[c] Institute of Geosciences, Shizuoka University, 836 Oya, Suruga, Shizuoka 422-8529, Japan
[d] Department of Earth Sciences, National Cheng Kung University, Tainan, Taiwan
[e] Research Center for Environmental Changes, Academia Sinica, Taipei, Taiwan

ARTICLE INFO

Keywords:
Seawater
Suspended particles
Clay minerals
Trace metals
Pacific Ocean
Marginal seas
GEOTRACES

ABSTRACT

Suspended particles are major carriers of trace metals in seawater, while the cycling mechanisms of particulate trace metals remain largely unclear owing to analytical challenges. In this study, we focused on the acid-leachability of particulate trace metals collected from the Pacific Ocean and investigated their compositional features by measuring the total dissolvable metal (tdM) and dissolved metal (dM) concentrations in unfiltered and filtered seawater samples, respectively. We defined the difference between total dissolvable and dissolved metals as the particulate metal (pM). We investigated the pM time course in acidified bottom waters (pH 1.9) over approximately two years. pM increased in two stages and reached equilibrium within a few years. In the field study, we stored acidified seawater samples at least two years before analysis. We compared pM with total particulate metal (tpM) concentrations in the same samples collected from 11 stations in the subarctic Pacific. The tpM concentrations were determined by particle filtration followed by total digestion using strong acids, including HF. The results indicate that pAl and pFe are nearly equivalent to tpAl and tpFe, respectively. Many metals in the suspended particles, including clay minerals, are highly acid-leachable during long-time storage. By compiling our pM data observed in the Pacific Ocean and its marginal seas (approximately 1500 samples), we found that the average pM/dM ratio across the Pacific is 9 for Al and 4 for Fe. Although pAl and pFe exhibit strong linear correlations, their concentrations and regression slopes are spatially variable, reflecting differences in sources and fluxes.

1. Introduction

The study of trace metals in seawater has advanced remarkably in recent decades owing to progress in analytical techniques and international collaboration through the GEOTRACES program (Anderson, 2024). However, trace metal speciation in seawater remains a major challenge. Marine particles are operationally and conventionally classified as either suspended or sinking particles (Roy-Barman and Jeandel, 2016; Twining, 2024). Sinking particles in the ocean have high settling velocities and are typically collected in situ using the sediment trap technique. Other approaches, such as in situ pumps equipped with large pore-size (50 μm) filters, are also employed to collect sinking particles. Suspended particles have low settling velocities and are usually collected on a membrane filter with a pore size of 0.2–0.45 μm from seawater that is collected with a sampling bottle or a pump. There are no theoretical threshold values for the settling velocities of the suspended and settling particles, and missing particles may exist between the suspended and settling particles (Misumi et al., 2021).

In this study, we focused on the suspended particles that form a fraction complementary to the dissolved fraction in seawater samples. The suspended particles are expected to be a complex mixture of lithogenic clay minerals (aluminosilicates), authigenic Fe—Mn oxyhydroxides, and biogenic phases such as carbonates, silica, and organic matter (Roy-Barman and Jeandel, 2016; Twining, 2024). The composition of these fractions should change spatially and temporally, and it is still a challenge to obtain the spatial and temporal dynamics. The

* Corresponding author.
E-mail addresses: sohrin@scl.kyoto-u.ac.jp (Y. Sohrin), zheng.linjie.7w@kyoto-u.ac.jp (L. Zheng), chan.cheukyin.y75@kyoto-u.ac.jp (C.-Y. Chan), nakaguch@chem.kindai.ac.jp (Y. Nakaguchi), takano.shotaro.3r@kyoto-u.ac.jp (S. Takano), sohrin.rumi@shizuoka.ac.jp (R. Sohrin), whliao@gs.ncku.edu.tw (W.-H. Liao), tyho@gate.sinica.edu.tw (T.-Y. Ho).

https://doi.org/10.1016/j.marchem.2025.104571
Received 9 May 2025; Received in revised form 29 July 2025; Accepted 7 October 2025
Available online 10 October 2025

formation of authigenic particles varies significantly across oceanic regions due to diverse sources and/or processes, including anthropogenic, hydrothermal, and volcanic inputs, and biological activity. In most cases, the metal elements in the suspended particles are dissolved in an aqueous solution prior to measurement. They are typically digested in concentrated strong acids containing HF to determine the total particulate metal (tpM) concentration (Twining, 2024). Many studies have assessed labile particulate metal (lpM) concentrations using mild extraction conditions, including acetic acid (Bruland et al., 1994), mixtures of acetic acid and reductant hydroxylamine hydrochloride (Berger et al., 2008), and mixtures of ligand ethylenediaminetetraacetic acid and reductant oxalic acid (Tovar-Sanchez et al., 2003), because lpM may be transformed into dissolved metal (dM) in seawater and might contribute to biological productivity. These methods commonly capture the biogenic and authigenic fractions of metals but generally excludes the lithogenic fraction (Rauschenberg and Twining, 2015). The difference between tpM and lpM is considered to represent the refractory particulate metal (rpM). However, oceanographic data for tpM, lpM, and rpM are limited compared to those for dM so far (Twining, 2024). This is mostly because the sampling and analysis of suspended particles are time-consuming, contamination cannot be easily prevented, and there is an inherent difficulty in intercalibration. The chemical nature of suspended particles has been examined in several studies (Ho et al., 2007; Lam et al., 2015; Planquette and Sherrell, 2012; Sherrell and Boyle, 1992; Twining et al., 2015). However, the effect of storage time on suspended and colloidal particles has been investigated in only a few cases (Jensen et al., 2020).

We employed an alternative method to measure particulate metal (pM). We determined total dissolvable metal (tdM) and dM concentrations using unfiltered and filtered seawater samples, respectively. Although tdM is defined in Sampling and Sample-Handling Protocols for GEOTRACES Cruises (GEOTRACES Standards and Intercalibration Committee, 2024), the effects of storage on tdM has not been sufficiently studied (Birchill et al., 2024; Michael et al., 2023; Seyitmuhammedov et al., 2022). In our previous studies, the unfiltered and filtered samples had been treated with HCl and preserved at a pH of approximately 2 for at least two years prior to analysis. The difference between tdM and dM concentrations was defined as the pM concentration. Using this method, we determined pM concentrations in the water columns of the North Pacific (Chan et al., 2024; Zheng et al., 2019; Zheng and Sohrin, 2019), the South Pacific (Zheng et al., 2022; Zheng et al., 2024), the East China Sea (Nakaguchi et al., 2021), the Seas of Japan and Okhotsk (Nakaguchi et al., 2022), and the Bering Sea (Cid et al., 2011). In these previous studies, we defined the difference between tdM and dM as lpM, because we had supposed that some fractions including aluminosilicates were not dissolved at pH ~2. Although a similar approach has been utilized in several studies (Evans and Nishioka, 2019; Lough et al., 2019; Munksgaard and Parry, 2001), there has been limiting understanding of what particulate fraction the tdM approach provides. The objective of this study is to explore the chemical nature of pM and to clarify the advantages and limitations of this approach. First, we present the time course of tdM, dM, and pM in the acidified bottom waters collected from coastal Japan and the western North Pacific. We then compare pM with tpM, determined using the same seawater samples collected from the same depths at 11 stations in the subarctic Pacific. Finally, we summarize our pM data from the Pacific Ocean and various marginal seas.

2. Material and methods

2.1. Time course of dM, tdM, and pM in acidified bottom seawater during storage

All materials were pre-cleaned with an alkaline detergent and acids (Minami et al., 2015). A bottom seawater sample was collected at the Suruga Bay Deep Seawater Aquaculture Research Center, where bottom seawater is continuously pumped through a rigid polyethene tube from a depth of 397 m, located 2.9 km offshore in Suruga Bay (35.850° N, 138.367° E; bottom depth 404 m) (Supplementary Fig. 1). Another bottom seawater sample was collected from a depth of 5222 m at station OP18 (41.000° N, 150.000° E; bottom depth 5253 m) during the Japanese GEOTRACES R/V Hakuho Maru KH-22-7 cruise using a clean sampling system (a carousel with Niskin-X bottles). Immediately after sampling, a part of seawater sample was filtered through an AcroPak 200 capsule filter with a pore size of 0.8/0.2 μm (Pall, USA). Filtered and unfiltered seawater samples were collected in separate 5 L polyethylene tanks (Rontainer, SEKISUI SEIKEI, Japan), amended with HCl (Optima, Thermo Fisher Scientific, USA) to be 0.02 mol/kg (pH 1.9), and stored at room temperature without shading. The bottles were shaken, and subsamples of approximately 100 g were taken from both filtered and unfiltered seawater at irregular intervals. Al, Mn, Fe, Co, Ni, Cu, Zn, Cd, and Pb in the subsamples were preconcentrated using a Nobias Chelate-PA1 resin column (Hitachi High Technologies, Japan). The unfiltered seawater was passed through a 0.45 μm pore-size syringe filter prior to being introduced into the resin column. The nine elements were determined with a high-resolution inductively coupled plasma mass spectrometer (HR-ICP-MS; Element 2; Thermo Fisher Scientific, USA) using calibration curves. Details of the analytical method are described in our previous paper (Minami et al., 2015). The pM concentration was obtained as the difference between the tdM and dM concentrations in units of nmol or pmol per kg of seawater.

2.2. Determination of pM and tpM in the subarctic Pacific seawater

We observed the distributions of tdM, dM, and pM in the subarctic Pacific at all stations during the Japanese GEOTRACES R/V Hakuho Maru KH-17-3 cruise. The seawater samples were acidified (pH 1.9) and preserved at room temperature for at least two years until analysis. The distributions of dM, tdM, and pM have been presented and discussed in previous studies (Chan et al., 2024; Chan et al., 2025).

Seawater samples for tpM were also collected at 11 stations during the KH17–3 cruise, using Niskin-X bottles that were different from those used for collecting tdM and dM samples (Supplementary Fig. 1). Firstly, 36 to 48 L of seawater were passed through the filtration device, which was equipped with 60 and 10 μm Nitex nets to collect size-fractionated suspended particles of >60 and 10–60 μm (Ho et al., 2007; Liao et al., 2017), and 5 to 10 L of seawater filtered through the 10 μm net was collected in a 10 L acid-cleaned low-density polyethylene carboy (Nalgene; Thermo Fisher Scientific, USA) for collecting particles in a fraction of 0.2–10 μm. The two large size-fractionated particles were then collected separately on a 10 μm polycarbonate membrane filter (Millipore; Merk, Germany) and the particles of 0.2–10 μm fraction were collected on a 0.2 μm polyethersulfone membrane filter (Sterlitech, USA). After filtration, the membranes were quickly rinsed with ultrapure water three times to remove seawater residue and decrease the interference of sea salts in the trace metal analysis. Membranes were sealed in 7 mL Teflon vials (Savillex, USA) and brought back to the laboratory in Taiwan. The membranes were digested with 5 mL of a mixture of 8 mol/kg HNO_3 and 2.9 mol/kg HF (J.T. Baker Ultrapure Acids; Avantor, USA) in Teflon vials at 120 °C on a hot plate for 12 h. After digestion, the residual liquids on the membranes were collected using ultrapure water. The elements in each digestion solution were determined using HR-ICP-MS (Element XR). The details of testing the precision, accuracy, and detection limits of the method for marine particle analysis are described in our previous papers (Liao and Ho, 2018; Liao et al., 2017). The tpM concentration was defined as the sum of the trace metal concentrations in the three size fractions (0.2–10, 10–60, and > 60 μm).

3. Results and discussion

3.1. Time course of dM, tdM, and pM in acidified bottom seawater during storage

The concentrations of dM, except dCu and dCo, were almost constant from the first day to the end of the experiment in the bottom waters of the western North Pacific (Fig. 1; Supplementary Table 1) and Suruga Bay (Supplementary Fig. 2; Supplementary Table 2). In contrast, dCu in Suruga Bay and dCo and dCu in the western North Pacific increased over time and reached a maximum within a few years. The concentrations of dAl, dMn, and dFe were 6–153 times higher in Suruga Bay bottom water than in the western North Pacific bottom water. Several studies have reported that dFe, dCu, dZn, dCd, and dCo form complexes with organic ligands in seawater (Moffett and Boiteau, 2024; Whitby et al., 2024). The stability constants and ligand concentrations were determined by indirect methods, such as competitive ligand exchange-adsorptive cathodic stripping voltammetry. The speciation of dFe is dominated by colloids based on filtration (Kunde et al., 2019). Colloidal contributions to dFe can vary considerably across ocean basins (Fitzsimmons et al., 2015). However, accurately identifying the specific compounds within organic complexes and colloids remains challenging with current analytical techniques. Our results suggest that most dM species are rapidly transformed at pH ~2 into forms that readily bind to the ethylenediaminetriacetic acid group of the Nobias Chelate-PA1 resin. For dCo and dCu, organic complexes are inert, and UV irradiation is necessary prior to preconcentration (Ruacho et al., 2022). The time courses of dCo and dCu could reflect the inertness of their organic complexes. These results for dM are consistent with previous reports (Milne et al., 2010).

In the bottom water of Suruga Bay, tdAl and tdFe were approximately 40 times higher than dAl and dFe, respectively, and increased more slowly than the td concentrations of the other elements (Supplementary Fig. 2). This is probably due to the dissolution of clay minerals,

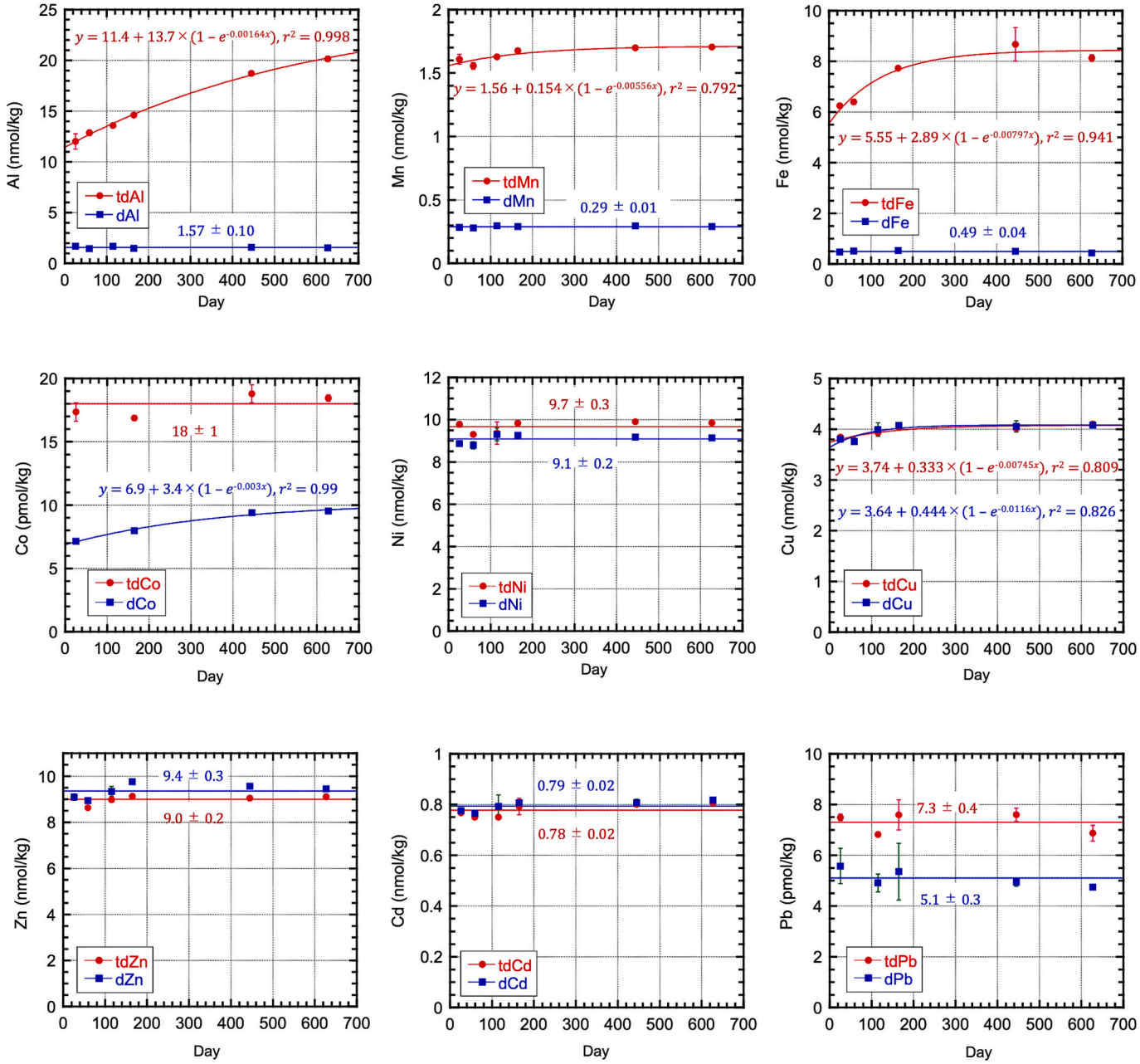

Fig. 1. Time course of mean tdM and dM at pH 1.9 in bottom water collected from the western North Pacific. The error bars represent ± sd.

which are a major fraction containing high concentrations of Al and Fe (Li, 2000). Significant differences between tdM and dM were also observed for Mn, Co, Cu, Zn, and Pb but not for Ni and Cd. In the western North Pacific bottom water, tdAl and tdFe were approximately 10 times higher than dAl and dFe, respectively, and increased more slowly than the td concentrations of the other elements (Fig. 1). Significant differences between tdM and dM were also observed for Mn, Co, and Pb but not for Ni, Cu, Zn, and Cd.

The resulting time courses for pAl, pMn, pFe, and pCo are shown in Fig. 2. The time courses of pPb and pCu in the bottom water of Suruga Bay are presented in Supplementary Fig. 3. We found that the increase in pM is a two-step process. Initially, the pM increased so rapidly that it was difficult to accurately track its time course under the experimental conditions of this study. Thus, we represent this fraction as pM_0, which may correspond to each element adsorbed onto the particulate surface. During the second step, pM increased more slowly with time. We assume that the subsequent increase in pM is caused by the dissolution of rpM in suspended particles and that the rate of decrease in rpM is proportional to the rpM concentration:

$$-\frac{d\mathrm{rpM}}{dt} = \lambda \mathrm{rpM}$$

where λ is an intrinsic constant for each element and each sample. Integration yields the following equation:

$$\mathrm{rpM} = \mathrm{rpM}_0 e^{-\lambda t}$$

where rpM_0 denotes the initial concentration. The total metal concentration in the suspended particles (tpM) is equal to the sum of pM_0 and rpM_0:

$$\mathrm{tpM} = \mathrm{pM}_0 + \mathrm{rpM}_0$$

Then, the measured pM is expressed as the following equation:

$$\mathrm{pM} = \mathrm{pM}_0 + \mathrm{rpM}_0 - \mathrm{rpM} = \mathrm{pM}_0 + \mathrm{rpM}_0\left(1 - e^{-\lambda t}\right)$$

This equation fits most of the pM time course data well. Although a longer observation period may have been desirable for pAl in the bottom water of Suruga Bay, we believe it is reasonable to assume a similar time course in this case. The time required for 90 % dissolution of rpM was: 571–1060 days for Al, 171–281 days for Fe, 11–181 days for Mn, and several–109 days for Co. Therefore, we propose that rpM, including aluminosilicates, is considerably more leachable than previously recognized and dissolves within a few years at approximately pH 2. Our hypothesis is as follows: aluminosilicates in suspended particles are primarily composed of clay minerals, which are prone to acid leaching due to their interlayers, where water molecules and hydrogen ions can penetrate (Grim, 1942).

As noted in the Introduction, many studies have evaluated lpM concentrations by extracting from suspended particles under various mild conditions using weak acids, reductants, and chelating ligands. It is possible that lpM determined by these methods is correlated with pM_0 in this study.

3.2. Comparison between pM and tpM in the subarctic Pacific seawater

As discussed above, pAl and pFe exhibited the highest concentrations in suspended particles and the lowest dissolution rates among the nine metals. Thus, we compared pAl and pFe with tpAl and tpFe, respectively, using data from the subarctic Pacific. Because the seawater samples for pM and tpM were collected using different Niskin-X bottles at the same time and depth during the same cast of the KH-17-3 cruise, they can be assumed to be identical with respect to dM.

pAl is linearly correlated with tpAl (Fig. 3). The slope of the regression is 0.935, close to unity. However, the *x*-axis intercept is positive, and the average pAl/tpAl ratio of the paired samples was 0.37 ± 0.32 (ave ± standard deviation (sd); $n = 56$). In particular, the pAl/

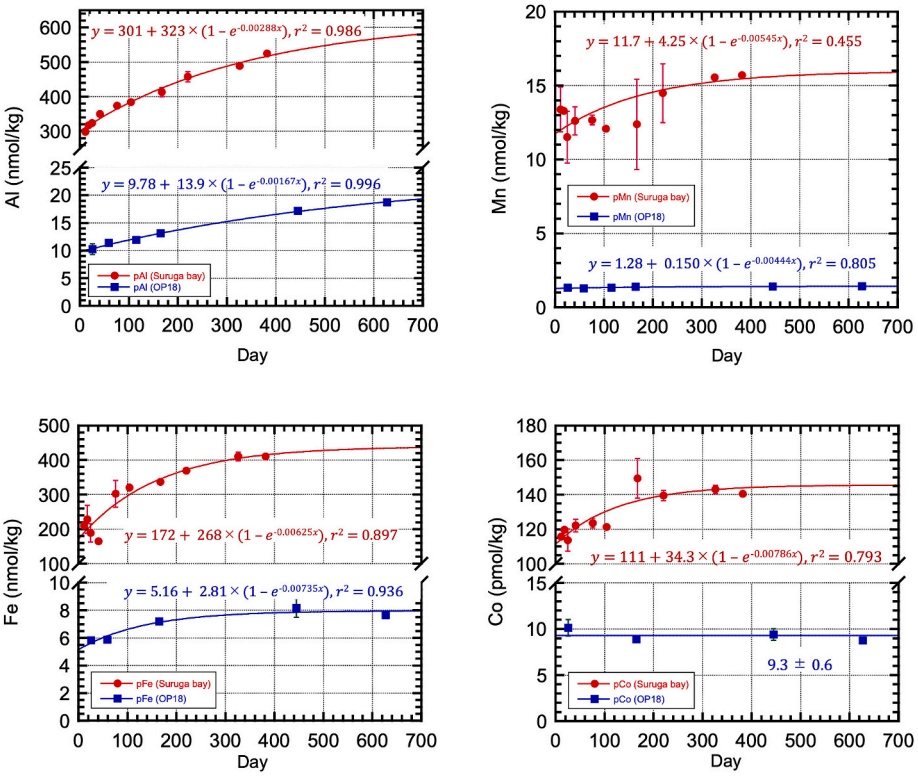

Fig. 2. Time course of mean pM concentrations in bottom water at pH 1.9 during storage. Red circles: coastal bottom water collected in Suruga Bay, Japan. Blue squares: western North Pacific bottom water. The error bars represent ± sd. (For interpretation of the references to colour in this figure legend, the reader is referred to the web version of this article.)

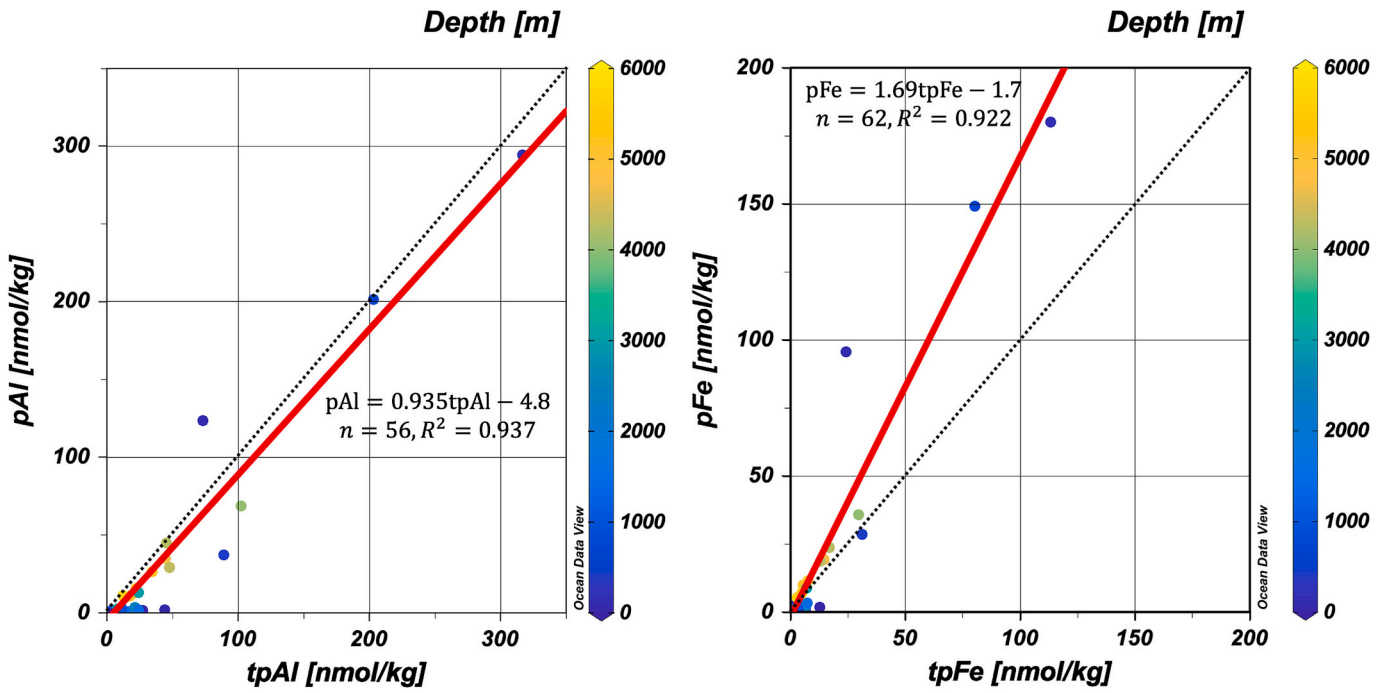

Fig. 3. Correlation between pAl and tpAl and between pFe and tpFe in seawater samples that were collected from the subarctic Pacific during the R/V Hakuho Maru KH-17-3 cruise. The red lines are obtained by linear regression. The doted lines represent 1:1 lines. The dot colour represents the sampling depth. (For interpretation of the references to colour in this figure legend, the reader is referred to the web version of this article.)

tpAl ratio was low in samples with low pAl (Supplementary Fig. 4). This is because that tpAl was higher than pAl, particularly when pAl was below 1 nmol/kg (Supplementary Fig. 5). For samples with pAl <1 nmol/kg, tpAl was relatively uniform at 2.8 ± 2.2 nmol/kg (n = 25). One possible explanation for these results is that the distribution of particles in seawater is not uniform, particularly in high-particle environments, resulting in differences in particulate matter between different Niskin bottles used for pM and tpM sampling. Second possibility is that certain minerals–such as feldspar, mica, biogenic silica, and zircon–may not dissolve effectively at a pH of approximately 2. Although such refractory minerals will not be major components in suspended particles, they may exist in seawater extensively at low concentrations. Another possibility is low-level contamination in tpAl, possibly at a few nmol/kg, during this cruise.

pFe is also linearly correlated with tpFe (Fig. 3). The slope of regression is 1.69, significantly higher than unity. When three data points with pFe > 50 nmol/kg were removed, the slope was 1.10. The high pFe was observed at station CL14 that is approximately 50 km off the Alaska coast, where substantially high dFe up to 5.2 nmol/kg was also observed. It is probable that the seawater samples from CL14 contained high concentrations of Fe—Mn oxyhydroxide colloids in addition to clay mineral particles. Small colloidal particles were not collected on the membrane filter during tpFe analysis. However, they may have been removed from the dFe samples during filtration with the depth filter (AcroPak 200 capsule), as the seawater samples were exposed to its large surface area. In this case, pFe contained small colloidal particles, which may have contributed to the steep slope observed in the pFe vs. tpFe relationship. In a similar manner with Al, the regression line of pFe vs. tpFe has a positive x-axis intercept. The pFe/tpFe ratio for each sample was 0.85 ± 0.70 (n = 62), being low for the samples with low pFe (Supplementary Fig. 4). tpFe was higher than pFe, particularly when pFe was below 0.5 nmol/kg (Supplementary Fig. 5). For samples with pFe < 0.5 nmol/kg, tpFe was relatively uniform at 1.1 ± 0.9 nmol/kg (n = 26). Again, possible explanations include the use of different Niskin bottles and the influence of refractory minerals. Alternatively, tpFe may have been contaminated at levels around 1 nmol/kg during this cruise.

These results indicate that pAl and pFe may serve as quantitative proxies for tpAl and tpFe, respectively, when concentrations are above a threshold and samples have been acidified for more than a few years for Al, and at least one year for Fe. Further study is necessary to make clear the differences between pAl and tpAl and between pFe and tpFe. Since the pM of the other elements is more acid-leachable than pAl and pFe, as shown in Section 3.1, this conclusion is also applicable to them.

3.3. Basin scale characteristics of pM

We observed the distribution of pM at 89 stations located in the North Pacific (Chan et al., 2024; Zheng et al., 2019; Zheng and Sohrin, 2019), the South Pacific (Zheng et al., 2022; Zheng et al., 2024), the East China Sea (Nakaguchi et al., 2021), the Seas of Japan and Okhotsk (Nakaguchi et al., 2022), and the Bering Sea (Cid et al., 2011) (Supplementary Figs. 6 and 7). Since the samples were stored at room temperature at approximately pH 2 for at least two years prior to analysis, pM was expected to be nearly equivalent to tpM. Here, we summarize the important results for pM.

The statistical data for pM and pM/dM in the Pacific Ocean are listed in Table 1. Since the relative standard deviation (rsd) for replicate analysis of the same sample was approximately 5 % for both tdM and dM at average seawater concentrations for all metals, the detection limit of pM was defined as twice the propagated uncertainty: $2 \times \sqrt{2} \times 0.05 \times C_{ave}$, where C_{ave} represents the average concentration of each dM in each cruise. One drawback of our method is that the detection limit of pM is relatively high, particularly for elements with low pM/dM ratios. pNi was not observed, whereas pZn and pCd were detected in only a few samples. Thus, our method is not so useful for nutrient-type trace metals in the Pacific Ocean. In contrast, the merit of our method is that the dM concentrations are intercalibrated using reference seawater materials (Minami et al., 2015; Sohrin et al., 2008). Additionally, dM and tdM were calibrated using the same working standard solutions. Thus, pM and dM can be compared at high precision. Most tpM samples are also analyzed in concert with particulate reference materials. However, the homogeneity of seawater reference materials is expected to be higher

Table 1
Statistical data of pM and pM/dM in the Pacific Ocean.

	Unit	Al	Mn	Fe	Co	Ni	Cu	Zn	Cd	Pb
pM										
detection limit	nmol/kg	0.06–0.3	0.05–0.1	0.06–0.1	(3–5) × 10^{-3}	0.9–1	0.2–0.3	0.6–1	0.07–0.1	(1–5) × 10^{-3}
n detected		935	943	1254	536	0	315	14	58	119
% detected		71	66	88	38	0	22	1	4	9
max	nmol/kg	381	6.7	211	9.2 × 10^{-2}		4.6	2.0	0.29	2.0 × 10^{-2}
min	nmol/kg	0.07	0.05	0.06	3 × 10^{-3}		0.2	0.69	0.11	1 × 10^{-3}
median	nmol/kg	1.17	0.16	0.64	5.4 × 10^{-3}		0.43	1.34	0.15	4.7 × 10^{-3}
ave*	nmol/kg	6	0.35	3	7.7 × 10^{-3}		0.49	1.3	0.15	4.9 × 10^{-3}
sd*	nmol/kg	24	0.68	14	8.3 × 10^{-3}		0.30	0.4	0.04	3.6 × 10^{-3}
pM/dM										
ave*		9	0.8	4	0.5		0.2			0.4
sd*		27	1.3	9	0.6		0.3			0.5

* Data below the detection limit were excluded from the calculations.

than that of oceanic particles. Furthermore, our method uses the same cartridge filter to separate d and p fractions, eliminating the risk of particulate loss between fractions. On average, pAl had the highest concentration, and its pAl/dAl ratio was the highest among the nine metals. This was followed by the pFe concentration and pFe/dFe ratio. The tpFe/dFe ratio has been reported to have a mean of 7.1, median of 1.9, and sd of 28 for the 1950 paired measurements in the GEOTRACES Intermediate Data Product 2021v2 (Twining, 2024). Our pFe/dFe ratio is consistent with the tpFe/dFe ratio, further supporting the idea that pFe is a good proxy for tpFe.

It should be noted that the ratios of pMn/dMn, pCo/dCo, and pPb/dPb are substantially lower than those of pAl/dAl and pFe/dFe. Because ave and sd were calculated based on detected concentrations, the actual pCo/dCo and pPb/dPb ratios would likely be lower if pCo and pPb values below the detection limit in this study were measurable. All five metals are classified as scavenged-type elements, and it has been assumed that dM is adsorbed onto particles and removed from the water column (Bruland and Lohan, 2003). The mechanism underlying the significant differences in pM/dM ratios of scavenged-type elements will be a subject of future study. In addition, the pCu/dCu ratio was comparable to the pCo/dCo and pPb/dPb ratios, implying that scavenging is an important factor for Cu. This finding is consistent with the conclusions of previous studies (Chan et al., 2025; Little et al., 2013; Takano et al., 2014; Zheng et al., 2021; Zheng et al., 2024).

A notable finding of this study is the strong basin-scale correlation between pFe and pAl. Fig. 4 shows the linear relationship between pFe and pAl over the pelagic Pacific Ocean. A map of the pelagic Pacific stations is shown in Supplementary Fig. 6. Furthermore, the linear relationship between pFe and pAl is a consistent feature across the Pacific and marginal seas, although the concentrations of pFe and pAl vary by more than two orders of magnitude (Table 2). The correlations between pFe and pAl in the marginal seas and off Alaska are presented in Supplementary Fig. 7.

The slopes of the regression lines increased in the following order: 0.25 for the East China Sea, 0.49 for the Sea of Japan, 0.54 for the pelagic Pacific, 0.58 for the Sea of Okhotsk, 0.63 for off Alaska, and 2.9 for the Bering Sea. The average pFe/pAl ratios for each sample were 0.7–2.4 times higher than the slopes but showed a similar order. The slopes and ratios were significantly higher than the average Fe/Al ratio of 0.23 in the upper crust (Rudnick and Gao, 2005). The high slopes and ratios in suspended particles imply the effects of biological uptake of dFe in the upper ocean and/or authigenesis of Fe—Mn oxyhydroxides in the water column of different oceanic regions. In addition, the spatial variations in the concentrations of pFe and pAl reflect the fluxes of Fe and Al into the ocean and seas. It is likely that the widespread presence of mafic and ultramafic complexes in Alaska (Patton Jr. et al., 1994), along with glaciation, are fundamental causes of the very high concentrations and ratios in the Bering Sea and off Alaska.

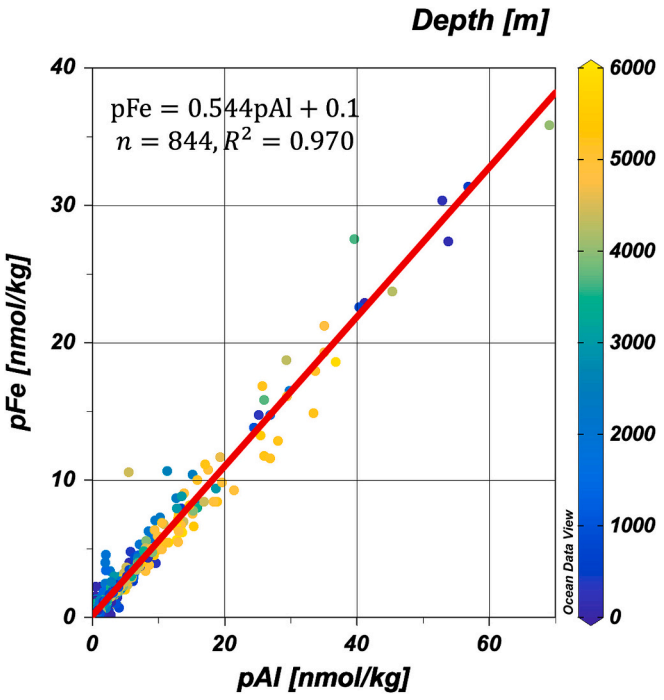

Fig. 4. Correlation between pFe and pAl over the pelagic Pacific Ocean. The red line is obtained by linear regression. The dot colour represents the sampling depth. (For interpretation of the references to colour in this figure legend, the reader is referred to the web version of this article.)

4. Conclusions

This study demonstrates that most metals can be effectively leached from suspended ocean particles when exposed to diluted HCl over a period of years. pM, determined as the difference between tdM and dM, is a good proxy for tpM that is determined via the strong acid digestion of particulate matter. The target acidification time will be a few years for pAl and one year for the other elements. The merits of our analysis for pM are as follows: the concentration of pM is related to the intercalibrated concentration of dM; approximately a hundred grams of filtered and unfiltered seawater subsampled from a sampling bottle are sufficient to determine pM; and the risk of contamination is low because strong acids at high concentrations are unnecessary. The drawbacks of this method are as follows: it is not very useful for elements with pM/dM < 0.1, because the detection limit of pM is relatively high due to the propagation of errors in tdM and dM; a time frame of year at approximately pH 2 is required for pM to reach an equilibrium concentration; colloid particles may be differently fractionated with depth and

Table 2
Regression line of pFe = *a*pAl + *b* and the pFe/pAl ratio in the Pacific Ocean and marginal seas.

	n	max pFe	max pAl	Regression line			pFe/pAl ratio		
		nmol/kg	nmol/kg	*a*	*b*	R^2	ave	±	sd
Pacific Ocean									
pelagic	844	36	69	0.544	0.1	0.970	0.70	±	0.48
off Alaska	49	211	381	0.628	2.8	0.982	0.90	±	1.12
East China Sea	34	760	2.87×10^3	0.246	11.7	0.799	0.58	±	0.34
Japan Sea	53	71	141	0.492	0.3	0.945	0.57	±	0.47
Okhotsk Sea	13	47	87	0.584	−2.3	0.994	0.43	±	0.18
Bering Sea	37	1.32×10^4	4.61×10^3	2.87	668	0.924	5.5	±	2.3

membrane filters; and metals contained in refractory minerals–such as feldspar, mica, biogenic silica, and zircon–cannot be accurately evaluated. pM can serve as a good proxy for tpM for Al, Mn, Fe, and Co in the open ocean. Additionally, pM of all nine elements can be observed in specific areas, such as the Bering Sea self (Cid et al., 2011).

In Sampling and Sample-handling Protocols for GEOTRACES Cruises (GEOTRACES Standards and Intercalibration Committee, 2024), it is stated that the samples for tdM should be acidified to pH 1.8 or 0.024 M HCl; however, no recommendations are provided regarding the storage time prior to analysis. Based on the results of this study, it is recommended that the samples should be stored for at least a few years for Al and at least one year for the other eight metals, to ensure reproducible determinations.

Our pM data from the Pacific and marginal seas revealed several novel results for metals in suspended particles. In seawater, the speciation of Al and Fe is primarily controlled by suspended particles, whereas that of Co and Pb is largely governed by dissolved species. pFe and pAl have a strong linear relationship over the Pacific Ocean and marginal seas, whereas the slope of pFe vs. pAl is unique to each region. To understand the biogeochemical cycles of trace metals, it is critical to clarify the interplay between dissolved, suspended, and settling particulate species. We hope that our methods and results contribute to future research.

CRediT authorship contribution statement

Yoshiki Sohrin: Writing – original draft, Supervision, Funding acquisition, Conceptualization. **Linjie Zheng:** Writing – review & editing, Investigation, Funding acquisition. **Cheuk-Yin Chan:** Writing – review & editing, Investigation, Funding acquisition. **Yuzuru Nakaguchi:** Writing – review & editing, Investigation, Funding acquisition. **Shotaro Takano:** Writing – review & editing, Resources. **Rumi Sohrin:** Writing – review & editing, Resources. **Wen-Hsuan Liao:** Writing – review & editing, Investigation. **Tung-Yuan Ho:** Writing – review & editing, Investigation, Funding acquisition.

Funding

This research was supported by the Japan Society for the Promotion of Science KAKENHI grants (19H01148 and 25 K03245 to YS; 21 K17877 to LZ), the Establishment of University Fellowships Towards the Creation of Science Technology Innovation, JST (JPMJFS2123 to CC), and the International Collaborative Research Program of the Institute for Chemical Research, Kyoto University (2024–55 and 2025–52 to TH; 2024–60 and 2025–58 to YN).

Declaration of competing interest

The authors declare that they have no known competing financial interests or personal relationships that could have appeared to influence the work reported in this paper.

Acknowledgements

We are grateful to the staff of the Suruga Bay Deep Seawater Aquaculture Research Center and the crew of the R/V Hakuho Maru for their assistance with seawater sampling. We also thank Editage (www.editage.jp) for English language editing.

Appendix A. Supplementary data

Supplementary data to this article can be found online at https://doi.org/10.1016/j.marchem.2025.104571.

Data availability

Data will be made available on request.

References

Anderson, R.F., 2024. GEOTRACES reflections. Oceanography 37 (2), 8–12. https://doi.org/10.5670/oceanog.2024.405.
Berger, C.J.M., Lippiatt, S.M., Lawrence, M.G., Bruland, K.W., 2008. Application of a chemical leach technique for estimating labile particulate aluminum, iron, and manganese in the Columbia River plume and coastal waters off Oregon and Washington. J. Geophys. Res. 113, C00B01. https://doi.org/10.1029/2007jc004703.
Birchill, A.J., et al., 2024. Pathways and timescales of Southern Ocean hydrothermal iron and manganese transport. Commun. Earth Environ 5 (1), 413. https://doi.org/10.1038/s43247-024-01564-8.
Bruland, K.W., Lohan, M.C., 2003. Controls of trace metals in seawater. In: Elderfield, H. (Ed.), The Oceans and Marine Geochemistry. Treatise on Geochemistry, Elsevier-Pergamon, Oxford, pp. 23–47.
Bruland, K.W., Orians, K.J., Cowen, J.P., 1994. Reactive trace metals in the stratified central North Pacific. Geochim. Cosmochim. Acta 58 (15), 3171–3182. https://doi.org/10.1016/0016-7037(94)90044-2.
Chan, C.-Y., Zheng, L., Sohrin, Y., 2024. The behaviour of aluminium, manganese, iron, cobalt, and lead in the subarctic Pacific Ocean: boundary scavenging and temporal changes. J. Oceanogr. 80 (2), 99–115. https://doi.org/10.1007/s10872-023-00710-8.
Chan, C.-Y., Zheng, L., Sohrin, Y., 2025. The behaviour of nickel, copper, zinc, and cadmium in the subarctic Pacific Ocean: East–West differences. J. Oceanogr. https://doi.org/10.1007/s10872-025-00746-y.
Cid, A.P., Urushihara, S., Minami, T., Norisuye, K., Sohrin, Y., 2011. Stoichiometry among bioactive trace metals in seawater on the Bering Sea shelf. J. Oceanogr. 67 (6), 747–764. https://doi.org/10.1007/s10872-011-0070-z.
Evans, L.K., Nishioka, J., 2019. Accumulation processes of trace metals into Arctic Sea ice: distribution of Fe, Mn and Cd associated with ice structure. Mar. Chem. 209, 36–47. https://doi.org/10.1016/j.marchem.2018.11.011.
Fitzsimmons, J.N., et al., 2015. Partitioning of dissolved iron and iron isotopes into soluble and colloidal phases along the GA03 GEOTRACES North Atlantic transect. Deep-Sea Res. II Top. Stud. Oceanogr. 116 (0), 130–151. https://doi.org/10.1016/j.dsr2.2014.11.014.
GEOTRACES Standards and Intercalibration Committee, 2024. Sampling and Sample-Handling Protocols for GEOTRACES Cruises. (version 4.0).
Grim, R.E., 1942. Modern concepts of clay materials. J. Geol. 50 (3), 225–275. https://doi.org/10.1086/625050.
Ho, T.-Y., Wen, L.-S., You, C.-F., Lee, D.-C., 2007. The trace metal composition of size-fractionated plankton in the South China Sea: biotic versus abiotic sources. Limnol. Oceanogr. 52 (5), 1776–1788. https://doi.org/10.4319/lo.2007.52.5.1776.
Jensen, L.T., Wyatt, N.J., Landing, W.M., Fitzsimmons, J.N., 2020. Assessment of the stability, sorption, and exchangeability of marine dissolved and colloidal metals. Mar. Chem. 220, 103754. https://doi.org/10.1016/j.marchem.2020.103754.

Kunde, K., et al., 2019. Iron distribution in the subtropical North Atlantic: the pivotal role of colloidal iron. Glob. Biogeochem. Cycles 33 (12), 1532–1547. https://doi.org/10.1029/2019GB006326.

Lam, P.J., Ohnemus, D.C., Auro, M.E., 2015. Size-fractionated major particle composition and concentrations from the US GEOTRACES North Atlantic zonal transect. Deep-Sea Res. II Top. Stud. Oceanogr. 116, 303–320. https://doi.org/10.1016/j.dsr2.2014.11.020.

Li, Y.-H., 2000. A Compendium of Geochemistry: from Solar Nebula to the Human Brain. Princeton University Press, Princeton, 475 pp.

Liao, W.-H., Ho, T.-Y., 2018. Particulate trace metal composition and sources in the Kuroshio adjacent to the East China Sea: the importance of aerosol deposition. J. Geophys. Res. Oceans 123 (9), 6207–6223. https://doi.org/10.1029/2018JC014113.

Liao, W.-H., Yang, S.-C., Ho, T.-Y., 2017. Trace metal composition of size-fractionated plankton in the Western Philippine Sea: the impact of anthropogenic aerosol deposition. Limnol. Oceanogr. 62 (5), 2243–2259. https://doi.org/10.1002/lno.10564.

Little, S.H., Vance, D., Siddall, M., Gasson, E., 2013. A modeling assessment of the role of reversible scavenging in controlling oceanic dissolved Cu and Zn distributions. Glob. Biogeochem. Cycles 27, 780–791. https://doi.org/10.1002/gbc.20073.

Lough, A.J.M., et al., 2019. Soluble iron conservation and colloidal iron dynamics in a hydrothermal plume. Chem. Geol. 511, 225–237. https://doi.org/10.1016/j.chemgeo.2019.01.001.

Michael, S.M., Crusius, J., Schroth, A.W., Campbell, R., Resing, J.A., 2023. Glacial meltwater and sediment resuspension can be important sources of dissolved and total dissolvable aluminum and manganese to coastal ocean surface waters. Limnol. Oceanogr. n/a (n/a). https://doi.org/10.1002/lno.12339.

Milne, A., Landing, W., Bizimis, M., Morton, P., 2010. Determination of Mn, Fe, Co, Ni, Cu, Zn, Cd and Pb in seawater using high resolution magnetic sector inductively coupled mass spectrometry (HR-ICP-MS). Anal. Chim. Acta 665 (2), 200–207. https://doi.org/10.1016/j.aca.2010.03.027.

Minami, T., et al., 2015. An off-line automated preconcentration system with ethylenediaminetriacetate chelating resin for the determination of trace metals in seawater by high-resolution inductively coupled plasma mass spectrometry. Anal. Chim. Acta 854, 183–190. https://doi.org/10.1016/j.aca.2014.11.016.

Misumi, K., et al., 2021. Slowly sinking particles underlie dissolved iron transport across the Pacific Ocean. Glob. Biogeochem. Cycles 35 (4), e2020GB006823. https://doi.org/10.1029/2020GB006823.

Moffett, J.W., Boiteau, R.M., 2024. Metal organic complexation in seawater: historical background and future directions. Annu. Rev. Mar. Sci. 16 (1), 577–599. https://doi.org/10.1146/annurev-marine-033023-083652.

Munksgaard, N.C., Parry, D.L., 2001. Trace metals, arsenic and lead isotopes in dissolved and particulate phases of north Australian coastal and estuarine seawater. Mar. Chem. 75 (3), 165–184. https://doi.org/10.1016/S0304-4203(01)00033-0.

Nakaguchi, Y., et al., 2021. Distribution and stoichiometry of Al, Mn, Fe, Co, Ni, Cu, Zn, Cd, and Pb in the East China Sea. J. Oceanogr. 77 (3), 463–485. https://doi.org/10.1007/s10872-020-00577-z.

Nakaguchi, Y., et al., 2022. Distribution and stoichiometry of Al, Mn, Fe, Co, Ni, Cu, Zn, Cd, and Pb in the Seas of Japan and Okhotsk. Mar. Chem. 241, 104108. https://doi.org/10.1016/j.marchem.2022.104108.

Patton Jr., W.W., Box, S.E., Grybeck, D.J., 1994. Ophiolites and other mafic-ultramafic complexes in Alaska. In: The Geology of Alaska. Geological Society of America, pp. 671–686.

Planquette, H., Sherrell, R.M., 2012. Sampling for particulate trace element determination using water sampling bottles: methodology and comparison to in situ pumps. Limnol. Oceanogr. Methods 10 (5), 367–388. https://doi.org/10.4319/lom.2012.10.367.

Rauschenberg, S., Twining, B.S., 2015. Evaluation of approaches to estimate biogenic particulate trace metals in the ocean. Mar. Chem. 171, 67–77. https://doi.org/10.1016/j.marchem.2015.01.004.

Roy-Barman, M., Jeandel, C., 2016. Marine Geochemistry. Oxford University Press, Oxford.

Ruacho, A., Richon, C., Whitby, H., Bundy, R.M., 2022. Sources, sinks, and cycling of dissolved organic copper binding ligands in the ocean. Commun. Earth Environ. 3 (1), 263. https://doi.org/10.1038/s43247-022-00597-1.

Rudnick, R.L., Gao, S., 2005. Composition of the continental crust. In: Rudnick, R.L. (Ed.), The Crust. Treatise on Geochemistry. Elsevier-Pergamon, Oxford, pp. 1–64.

Seyitmuhammedov, K., et al., 2022. The distribution of Fe across the shelf of the Western Antarctic Peninsula at the start of the phytoplankton growing season. Mar. Chem. 238, 104066. https://doi.org/10.1016/j.marchem.2021.104066.

Sherrell, R.M., Boyle, E.A., 1992. The trace metal composition of suspended particles in the oceanic water column near Bermuda. Earth Planet. Sci. Lett. 111 (1), 155–174. https://doi.org/10.1016/0012-821X(92)90176-V.

Sohrin, Y., et al., 2008. Multielemental determination of GEOTRACES key trace metals in seawater by ICPMS after preconcentration using an ethylenediaminetriacetic acid chelating resin. Anal. Chem. 80 (16), 6267–6273. https://doi.org/10.1021/ac800500f.

Takano, S., Tanimizu, M., Hirata, T., Sohrin, Y., 2014. Isotopic constraints on biogeochemical cycling of copper in the ocean. Nat. Commun. 5, 5663. https://doi.org/10.1038/ncomms6663.

Tovar-Sanchez, A., et al., 2003. A trace metal clean reagent to remove surface-bound iron from marine phytoplankton. Mar. Chem. 82 (1), 91–99. https://doi.org/10.1016/S0304-4203(03)00054-9.

Twining, B.S., 2024. An ocean of particles characterization of particulate trace elements by the GEOTRACES program. Oceanography 37 (2), 120–130. https://doi.org/10.5670/oceanog.2024.407.

Twining, B.S., Rauschenberg, S., Morton, P.L., Vogt, S., 2015. Metal contents of phytoplankton and labile particulate material in the North Atlantic Ocean. Prog. Oceanogr. 137, Part A, 261–283. https://doi.org/10.1016/j.pocean.2015.07.001.

Whitby, H., et al., 2024. New insights into the organic complexation of bioactive trace metals in the global ocean from the geotraces era. Oceanography 37 (2), 142–155. https://doi.org/10.5670/oceanog.2024.419.

Zheng, L., Sohrin, Y., 2019. Major lithogenic contributions to the distribution and budget of iron in the North Pacific Ocean. Sci. Rep. 9 (1), 11652. https://doi.org/10.1038/s41598-019-48035-1.

Zheng, L., et al., 2019. Distinct basin-scale-distributions of aluminum, manganese, cobalt, and lead in the North Pacific Ocean. Geochim. Cosmochim. Acta 254, 102–121. https://doi.org/10.1016/j.gca.2019.03.038.

Zheng, L., Minami, T., Takano, S., Ho, T.-Y., Sohrin, Y., 2021. Sectional distribution patterns of Cd, Ni, Zn, and Cu in the North Pacific Ocean: relationships to nutrients and importance of scavenging. Glob. Biogeochem. Cycles 35 (7), e2020GB006558. https://doi.org/10.1029/2020GB006558.

Zheng, L., Minami, T., Takano, S., Sohrin, Y., 2022. Distributions of aluminum, manganese, cobalt, and lead in the western South Pacific: interplay between the South and North Pacific. Geochim. Cosmochim. Acta 338, 105–120. https://doi.org/10.1016/j.gca.2022.10.022.

Zheng, L., Minami, T., Takano, S., Sohrin, Y., 2024. Distributions of cadmium, nickel, zinc, copper, and iron in the western South Pacific Ocean: local sources of the nutrient-type trace metals. Mar. Chem. 263-264, 104411. https://doi.org/10.1016/j.marchem.2024.104411.